Progress In Electromagnetics Research B, Vol. 66, 49–61, 2016

Electromagnetic Field Theory for Invariant Beams Using Scalar Potentials

Irving Rondón-Ojeda* and Francisco Soto-Eguibar

Abstract—We present a description of the electromagnetic field for propagation invariant beams using scalar potentials. Fundamental dynamical quantities are obtained: energy density, Poynting vector and Maxwell stress tensor. As an example, all these quantities are explicitly calculated for the Bessel beams, which are invariant beams with circular cylindrical symmetry.

1. INTRODUCTION

Propagation invariant beams, also known as "non-diffracting beams", propagate indefinitely without changing their transverse intensity distribution. These optical fields are well-known plane waves, the Bessel beams [1], Mathieu beams [2] and Weber beams [3]. These invariant beams correspond to the solutions of the Helmholtz wave equation in Cartesian, circular cylindrical, parabolic cylindrical, and elliptical cylindrical coordinates, respectively. These non-diffracting beams have a large quantity of applications in fundamental and applied science in areas such as quantum mechanics [4–7], acousto-optics [8], nonlinear optics [9], optical tweezers [10], fluid dynamics [11], and optical communications [12], among others.

In order to obtain the maximum possible information from these fields, it is very important to have a deeper insight of their physical properties. Although the vector approach is the most common method used in electromagnetic theory, several interesting works have used a scalar formalism [1], such as [13] and [14]. We use scalar approach in order to obtain the fundamental dynamic quantities of those beams; dynamic quantities are present in several physical phenomena which occur in different contexts and scenarios, but are nevertheless governed by the same physical laws. To the best of our knowledge, the complete general explicit expressions have not been presented before; as a matter of fact, the Maxwell stress tensor has been scarcely mentioned in the previously published literature. Additionally, by considering the interference between modes, our results can give new insights.

It must be emphasized that the scalar potential approach and more general vector approach are completely equivalent, in the understanding that the results predicted for the measured quantities are exactly the same in both approaches; however, in several circumstances, such as the one presented here, the scalar approach is easier. The link between these two approaches is the Hertz potential formalism [15], but a review of this is beyond the scope of this paper.

The article is organized as follows: In Section 2, starting from the Maxwell equations, we present the scalar potential approach. Then, an exact explicit expression, in terms of the scalar potential, is derived for the energy density of the invariant fields in Section 3, and the same is done for the Poynting vector in Section 4. In Section 5, the Maxwell stress tensor is calculated. In order to present concrete examples, we have evaluated the corresponding quantities for the Bessel beams in each section. To show the usefulnesses of the method, in Section 6, the force exerted by a zero order Bessel beam on a

Received 31 December 2015, Accepted 8 February 2016, Scheduled 16 February 2016

* Corresponding author: Irving Rondon-Ojeda (irondon@inaoep.mx).

The authors are with the Instituto Nacional de Astrofísica Óptica y Electrónica, Puebla, Luis Enrique Erro 1, Santa María Tonantzintla, San Andrés Cholula, Puebla 72840, México.

small cylinder is calculated using the Maxwell stress tensor. Finally, our conclusions are presented in Section 7.

2. SCALAR POTENTIALS

Any given electromagnetic field answers to the Maxwell equations, which in the International System of Units (SI) [15–17] are

$$\nabla \cdot \vec{D} = \rho_f, \tag{1a}$$

$$\nabla \cdot \vec{B} = 0, \tag{1b}$$

$$\nabla \times \vec{E} = -\frac{\partial \vec{B}}{\partial t}, \tag{1c}$$

$$\nabla \times \vec{H} = \vec{J}_f + \frac{\partial \vec{D}}{\partial t}, \tag{1d}$$

where the microscopic electric and magnetic fields are $\vec{E}$ and $\vec{B}$; the corresponding macroscopic fields are $\vec{D}$ and $\vec{H}$; ρ_f is the free charge density; $\vec{J}_f$ is the free current density.

The constitutive relations between micro and macroscopic vector fields are

$$\vec{D} = \varepsilon_0 \vec{E} + \vec{P}, \tag{2a}$$

$$\vec{B} = \mu_0 \left(\vec{H} + \vec{M} \right), \tag{2b}$$

where the electric polarization, $\vec{P}$, is the average electric dipole moment per unit volume, and the magnetization, $\vec{M}$, is the average magnetic dipole moment per unit volume; the free-space electric permittivity is ε_0, and μ_0 is the free space magnetic permeability.

For the sake of simplicity, we will consider an isotropic linear homogeneous medium without losses, which means that the electric permittivity ε and magnetic susceptibility μ are both real constants; hence, the constitutive relations reduce to $\vec{D} = \varepsilon \vec{E}$ and $\vec{B} = \mu \vec{H}$. As we are interested only in the propagation of the electromagnetic fields and not in its production, we will also suppose that there is no free charge density nor free currents. Without loss of generality, we will also suppose that all the fields are monochromatic, of frequency ω. With all these considerations, we can rewrite the Maxwell equations as

$$\nabla \cdot \vec{E} = 0, \tag{3a}$$

$$\nabla \cdot \vec{H} = 0, \tag{3b}$$

$$\nabla \times \vec{E} = -i\omega\mu \vec{H}, \tag{3c}$$

$$\nabla \times \vec{H} = i\omega\varepsilon \vec{E}. \tag{3d}$$

If we take the curl of Equations (3c) and (3d), and combine with the other two Maxwell equations, we obtain the Helmholtz vector equations for the electric field and for the magnetic field,

$$\nabla^2 \vec{E} + k^2 \vec{E} = 0, \tag{4a}$$

$$\nabla^2 \vec{H} + k^2 \vec{H} = 0, \tag{4b}$$

where we have defined the wave-vector magnitude $k^2 = (\omega/v)^2$ in terms of the speed of light in the medium, $v^2 = \frac{1}{\mu\varepsilon}$.

Let us write the electromagnetic fields as [15]

$$\vec{E} = c_{\mathrm{TE}} \vec{M}(\vec{r}) + c_{\mathrm{TM}} \vec{N}(\vec{r}), \tag{5a}$$

$$\vec{H} = -i\sqrt{\frac{\varepsilon}{\mu}} \left[c_{\mathrm{TE}} \vec{N}(\vec{r}) + c_{\mathrm{TM}} \vec{M}(\vec{r}) \right], \tag{5b}$$

being $\vec{M}(\vec{r})$ and $\vec{N}(\vec{r})$ vector fields defined by

$$\vec{M}(\vec{r}) = \nabla \times [\hat{a}\psi(\vec{r})] \tag{6}$$

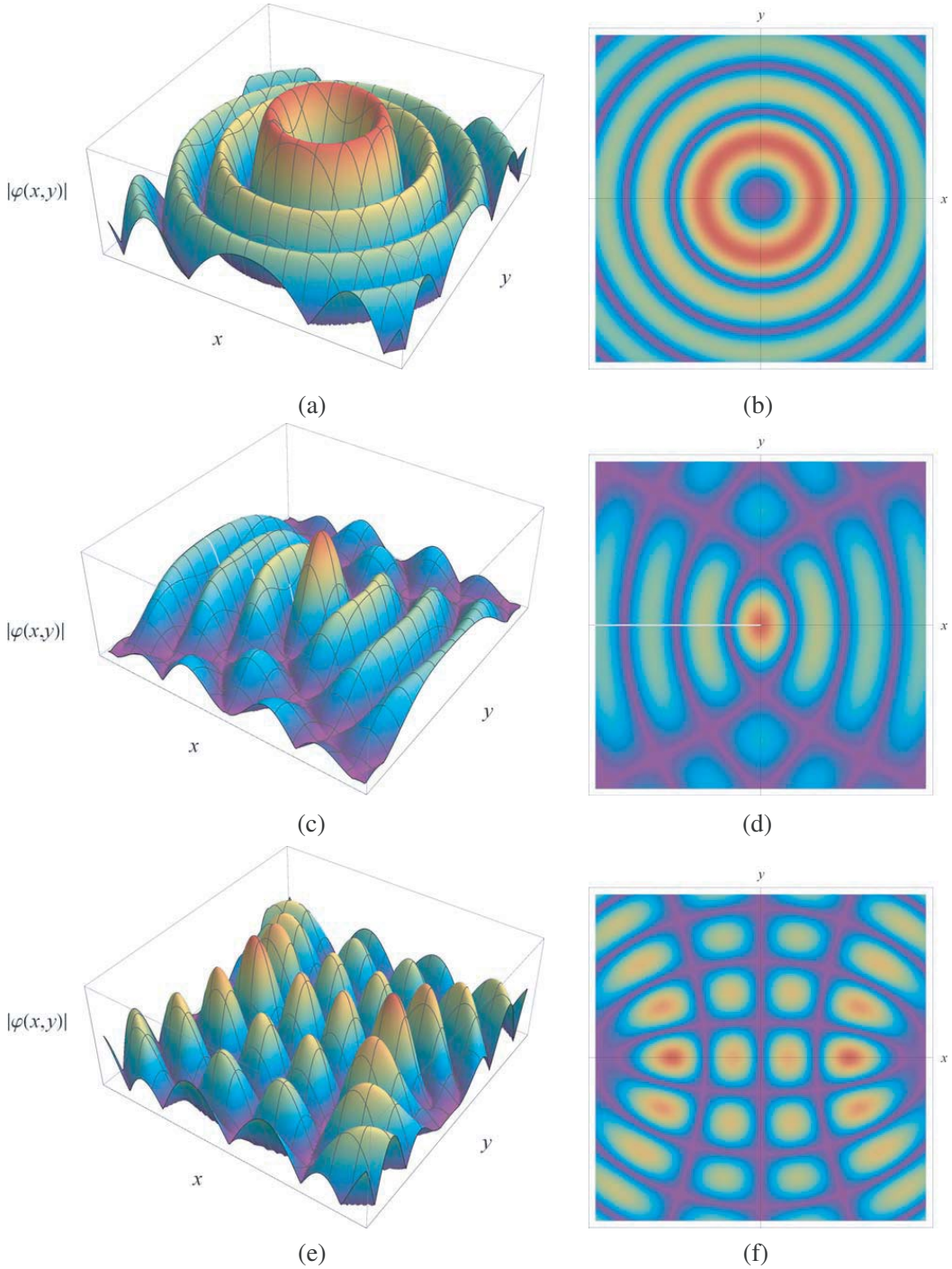

Figure 1. Absolute value of the solution of the transversal Hemholtz Equation (10). In all graphics, we have used $k_T = 1\,\mathrm{m}^{-1}$. The scalar potential φ is given in volts. (a) Cylindrical coordinates: A Bessel beam with $\upsilon = 3$. (c) Parabolic cylindrical coordinates: An even Weber beam with $a = 0$. (e) Elliptical cylindrical coordinates: An even Mathieu beam with $q = 25$, $n = 3$ and $f = 2\sqrt{q} = 11.28$.

and

$$\vec{N}(\vec{r}) = \frac{1}{k}\nabla \times \vec{M}(\vec{r}), \tag{7}$$

where $\hat{a}$ is an arbitrary unit vector; c_{TE} and c_{TM} are two arbitrary complex numbers (the TE and TM

sub indexes will be justified below); $\psi(\vec{r})$ is a scalar field.

It is straightforward to verify that if the scalar field $\psi(\vec{r})$ satisfies the scalar Helmholtz equation,

$$\nabla^2\psi + k^2\psi = 0, \tag{8}$$

then the fields (5a) and (5b) satisfy the vector Helmholtz equation. So, the scalar field $\psi(\vec{r})$ will be named scalar potential. Note that these new vector fields, $\vec{M}$ and $\vec{N}$, are orthogonal between them, that is $\vec{M}\cdot\vec{N} = 0$, and solenoidal, i.e., $\nabla\cdot\vec{M} = 0$ and $\nabla\cdot\vec{N} = 0$.

Though the homogeneous (source-free) Helmholtz equation can be separated in eleven coordinate systems, we require separability into transverse and longitudinal parts and that is possible only in Cartesian, cylindrical, parabolic cylindrical and elliptical cylindrical coordinates [18]. The spatial evolution of the scalar potential ψ can then be described by the transverse and the longitudinal parts; the transverse part $\varphi(u_1, u_2)$ will depend only on the transverse coordinates, u_1, u_2, and the longitudinal part $Z(z)$ will depend on the longitudinal coordinate z; thus

$$\psi(u, v, z) = \varphi(u_1, u_2)Z(z). \tag{9}$$

After substituting Eq. (9) in the Helmholtz equation, we easily obtain that $\varphi(u_1, u_2)$ satisfy the two-dimensional transverse Helmholtz equation

$$\nabla_T^2\varphi + k_T^2\varphi = 0, \tag{10}$$

where ∇_T^2 is the Laplacian transversal operator, which has a specific form in each coordinate system, and the longitudinal part is $Z(z) = e^{ik_z z}$, with the dispersion relation $k^2 = k_T^2 + k_z^2$. In Figure 1, we show the transversal field distribution, given by the solution of (10), for cylindrical, parabolic cylindrical and elliptical cylindrical coordinates. To enhance the knowledge on these fields, we refer the reader to [19–21] for a general description, physical properties, experiments and applications, and for recent advances to [22].

We choose the unit vector $\hat{a}$, in Equation (6), as the unit vector that determines the direction of propagation, i.e., the Z axis, and we note that in the four coordinate systems the scale factor h_3 that we are studying is equal to 1, to write

$$\vec{M} = -e^{ik_z z}\nabla_T^{\perp}\varphi, \tag{11}$$

where

$$\nabla_T^{\perp} = -\hat{e}_1\frac{1}{h_2}\frac{\partial}{\partial u_2} + \hat{e}_2\frac{1}{h_1}\frac{\partial}{\partial u_1}, \tag{12}$$

$\hat{e}_1$ and $\hat{e}_2$ are the base unit vectors corresponding to the transversal direction, and h_1 and h_2 are the corresponding scale factors. It is also very easy to see that

$$\vec{N} = \frac{e^{ik_z z}}{k}\left(ik_z\nabla_T + \hat{e}_3 k_T^2\right)\varphi, \tag{13}$$

where

$$\nabla_T = \hat{e}_1\frac{1}{h_1}\frac{\partial}{\partial u_1} + \hat{e}_2\frac{1}{h_2}\frac{\partial}{\partial u_2}. \tag{14}$$

2.1. Example Bessel TE and TM Modes

Since their introduction in 1987 by Durnin [1], the Bessel beams have attracted considerable attention due to their properties of propagation invariance and self-reconstruction, and they have found a wide range of interesting applications; for a historical review see [23], for experimental mode realizations [24] and for the vectorial approach [25–27]. Thus, as an example, we consider the case of the Bessel beams, which correspond to write the scalar transversal Helmholtz equation (10) in cylindrical coordinates. In this instance, the solution is

$$\varphi(r, \theta) = J_\nu\left(k_T r\right)e^{i\nu\theta}, \tag{15}$$

where ν is a non-negative integer and $J_\nu(\zeta)$ a Bessel function of the first kind of order ν.

Let us substitute (15) and set $c_{\mathrm{TM}} = 0$, $c_{\mathrm{TE}} = 1$ in Equation (5), to find

$$\vec{E}^{TE} = \mathrm{Re}\left(\frac{1}{r}\left\{i\nu J_\nu(k_T r)\hat{e}_r + [\nu J_\nu(k_T r) - k_T r J_{\nu-1}(k_T r)]\,\hat{e}_\theta\right\} e^{i\nu\theta} e^{ik_z z}\right), \tag{16}$$

and

$$\vec{H}^{TE} = \mathrm{Re}\left(\sqrt{\frac{\varepsilon}{\mu}}\frac{1}{2kr}\left\{rk_T k_z[J_{\nu-1}(rk_T) - J_{\nu+1}(rk_T)]\hat{e}_r + 2i\nu k_z J_\nu(rk_T)\,\hat{e}_\theta - 2irk_T^2 J_\nu(rk_T)\hat{e}_z\right\} e^{i\nu\theta} e^{ik_z z}\right), \tag{17}$$

being $\hat{e}_r$, $\hat{e}_\theta$, $\hat{e}_z$ the unit base vectors in cylindrical coordinates. Note that the electric field is transversal, which means that its component in the propagation direction, Z, is zero. This justifies *a posteriori* the notation, the TE as super index in the electromagnetic fields and as subindex in the constant c_{TE}.

We substitute again (15) in Equation (5), but we make now $c_{\mathrm{TE}} = 0,\ c_{\mathrm{TM}} = 1$, to find

$$\vec{E}^{TM} = \mathrm{Re}\left(\frac{1}{kr}\left\{ik_z\left[rk_T J_{\nu-1}(rk_T) - \nu J_\nu(rk_T)\right]\hat{e}_r - \nu k_z J_\nu(rk_T)\,\hat{e}_\theta + rk_T^2 J_\nu(rk_T)\,\hat{e}_z\right\} e^{i\nu\theta} e^{ik_z z}\right), \tag{18}$$

and

$$\vec{H}^{TM} = \mathrm{Re}\left(\sqrt{\frac{\varepsilon}{\mu}}\frac{1}{2r}\left\{2\nu J_\nu(rk_T)\,\hat{e}_r + irk_T\left[J_{\nu-1}(rk_T) - J_{\nu+1}(rk_T)\right]\hat{e}_\theta\right\} e^{i\nu\theta} e^{ik_z z}\right). \tag{19}$$

Note now that the magnetic field is transversal, which is the reason that we use TM as super index in the electromagnetic field and as subindex in the constant c_{TM}.

Thus, in general, when $c_{\mathrm{TE}} = 1$ and $c_{\mathrm{TM}} = 0$ in Equation (5), we will get a transverse electric wave, and when $c_{\mathrm{TE}} = 0$ and $c_{\mathrm{TM}} = 1$ in Equation (5), we will get a transverse magnetic wave.

3. ELECTROMAGNETIC ENERGY DENSITY

The time averaged electromagnetic energy density $\langle\mathcal{U}\rangle$ for an harmonic field in an isotropic, linear and homogeneous medium is given by [15–17]

$$\langle\mathcal{U}\rangle = \frac{1}{4}\mathrm{Re}\left(\varepsilon\vec{E}\cdot\vec{E}^* + \mu\vec{H}\cdot\vec{H}^*\right), \tag{20}$$

where the upper index $*$ stands for the complex conjugate. Inserting the vector fields $\vec{M}$ and $\vec{N}$ in this formula, we obtain

$$\langle\mathcal{U}\rangle \;\; = \left(|c_{\mathrm{TE}}|^2 + |c_{\mathrm{TM}}|^2\right)\left(\langle\mathcal{U}\rangle_{\mathrm{tra}} + \langle\mathcal{U}\rangle_{\mathrm{z}}\right) + \langle\mathcal{U}\rangle_{\mathrm{int}} \tag{21}$$

where

$$\langle\mathcal{U}\rangle_{\mathrm{tra}} = \frac{\varepsilon}{4}\left(1 + \frac{k_z^2}{k^2}\right)\mathrm{Re}\left(\nabla_T\varphi\cdot\nabla_T\varphi^*\right), \tag{22}$$

$$\langle\mathcal{U}\rangle_{\mathrm{z}} = \frac{\varepsilon}{4}\frac{k_T^4}{k^2}\varphi\varphi^* \tag{23}$$

and

$$\langle\mathcal{U}\rangle_{\mathrm{int}} = \varepsilon\frac{k_z}{2k}\,\mathrm{Re}\left[i\left(c_{\mathrm{TE}}\,c_{\mathrm{TM}}^* + c_{\mathrm{TE}}^*\,c_{\mathrm{TM}}\right)\left(\nabla_T^{\perp}\varphi\cdot\nabla_T\varphi^*\right)\right]. \tag{24}$$

The first term in (21) is the energy of the transverse and longitudinal fields, and (24) is the energy of the "interference" between the electric transversal modes and the magnetic transversal modes. We observe that the transversal electric and magnetic fields have the same energy, but there is an interference term, which in general, will be different from zero, as the author of [28] noted studying the Poynting vector. It is worth to note that the expression reported here is valid for any invariant field and that the time averaged energy density does not depend on the longitudinal variable z, as must be.

3.1. Energy Density for Bessel Beams

In the case of Bessel beams of order ν, the transversal energy density is

$$\langle \mathcal{U} \rangle_{\text{tra}} = \frac{\varepsilon}{4k^2r^2}\Big\{ J_\nu^2(rk_T)\left[2\nu^2\left(k^2+k_z^2\right)+r^2k_T^4\right]+r^2k_T^2\left(k^2+k_z^2\right)J_{\nu-1}^2(rk_T) \\ -2\nu r k_T\left(k^2+k_z^2\right)J_{\nu-1}(rk_T)J_\nu(rk_T)\Big\}, \tag{25}$$

and the interference energy density is

$$\langle \mathcal{U} \rangle_{\text{int}} = \frac{\varepsilon k_z}{kr^2}\text{Re}\left\{\left(c_{\text{TE}}c_{\text{TM}}^* + c_{\text{TE}}^*c_{\text{TM}}\right)\nu J_\nu(rk_T)\left[rk_TJ_{\nu-1}(rk_T)-\nu J_\nu(rk_T)\right]\right\}. \tag{26}$$

When $\nu = 0$, i.e., for a Bessel beam of zero order, the total energy density is simplified to

$$\langle \mathcal{U} \rangle = \frac{\varepsilon k_T^2}{4k^2}\left(|c_{\text{TE}}|^2+|c_{\text{TM}}|^2\right)\left[k_T^2J_0^2(k_Tr)+\left(k^2+k_z^2\right)J_1^2(k_Tr)\right], \tag{27}$$

where physically the first term is related to the longitudinal component and the second one due to the transversal fields; similar expressions were reported by [25–27]. We want to remark that choosing appropriate c_{TE} and c_{TM} can lead to an linearly polarized Bessel beam with total angular momentum equal to the order of the Bessel function as linearly polarized basis does not carry orbital angular momentum. In the same manner, if c_{TE} and c_{TM} are chosen to deliver a right or left circularly polarized basis, for a Bessel field of total orbital angular momentum ν, the Bessel functions will have an order $\nu - 1$ and $\nu + 1$ as circularly polarized basis carries orbital angular momentum plus one and orbital angular momentum minus one [13]. In this work, we decide to focus on TEM modes.

Note that in the case of a Bessel beam of zero order, the interference part is null. In Figure 2, we show the total energy density for a Bessel beam with $\nu = 0$. Remark also that Bessel beams have the energy distributed between the rings, so that the more rings they have, the lower is the energy in the central core, and this is important in many experimental applications (an interesting theoretical and experimental study was reported in [29]).

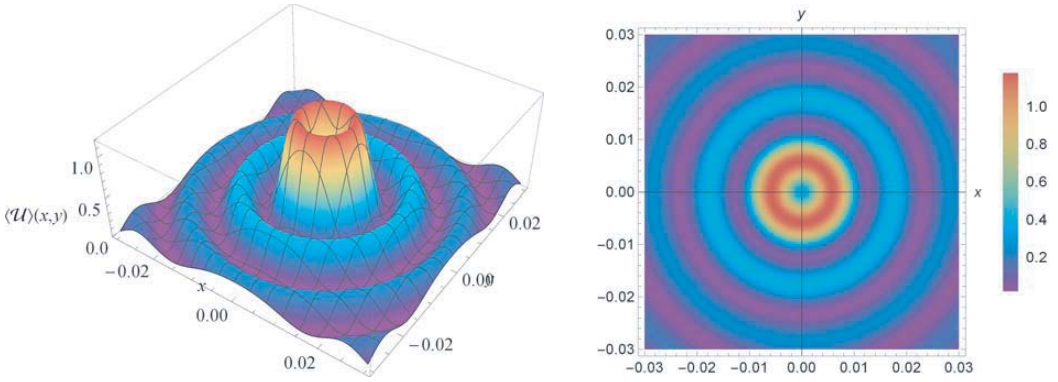

Figure 2. The energy density, given by Equation (27), for a TE Bessel beam with $\nu = 0$, $k = 630\,\text{m}^{-1}$ and $k_T = 300\,\text{m}^{-1}$.

4. POYNTING VECTOR

For harmonic electromagnetic fields, the time average power flow per unit area is given by [15–17]

$$\left\langle \vec{S} \right\rangle = \frac{1}{2}\text{Re}\left(\vec{E}\times\vec{H}^*\right). \tag{28}$$

Following the same procedure that is in the energy density case in the previous section and after performing the algebra, we obtain

$$\left\langle \vec{S} \right\rangle = |c_{\text{TE}}|^2\left\langle \vec{S}_{\text{TE}} \right\rangle + |c_{\text{TM}}|^2\left\langle \vec{S}_{\text{TM}} \right\rangle + \left\langle \vec{S}_{\text{int}} \right\rangle, \tag{29}$$

where

$$\left\langle \vec{S}_{\mathrm{TE}} \right\rangle = \frac{1}{2k}\sqrt{\frac{\varepsilon}{\mu}}\mathrm{Re}\left[\left(\nabla_T\varphi\cdot\nabla_T\varphi^*\right)k_z\hat{e}_3 - ik_T^2\,\varphi^*\,\nabla_T\varphi\right] \tag{30}$$

is the transversal electric part, and

$$\left\langle \vec{S}_{\mathrm{TM}} \right\rangle = \frac{1}{2k}\sqrt{\frac{\varepsilon}{\mu}}\mathrm{Re}\left[\left(\nabla_T\varphi\cdot\nabla_T\varphi^*\right)k_z\hat{e}_3 + ik_T^2\,\varphi^*\,\nabla_T\varphi\right] \tag{31}$$

is the transversal magnetic part, and

$$\left\langle \vec{S}_{\mathrm{int}} \right\rangle = \frac{1}{2k^2}\sqrt{\frac{\varepsilon}{\mu}}\mathrm{Re}\left[i\left(c_{\mathrm{TE}}\,c_{\mathrm{TM}}^*k^2 + c_{\mathrm{TE}}^*\,c_{\mathrm{TM}}k_z^2\right)\left(\nabla_T^{\perp}\varphi\cdot\nabla_T\varphi^*\right)\hat{e}_3 + c_{\mathrm{TE}}^*\,c_{\mathrm{TM}}k_zk_T^2\,\nabla_T^{\perp}\left(\varphi\varphi^*\right)\right] \tag{32}$$

is the interference part, which in general is not zero. Notice that this time averaged Poynting vector is independent of the z coordinate, as expected.

In order to emphasizes the non-diffractive character of these beams, it is shown that the divergence of the transversal part of the time averaged Poynting vector is zero. To make this fact evident, let us write the time averaged Poynting vector as a sum of a transversal and a longitudinal part as

$$\left\langle \vec{S} \right\rangle = \left\langle \vec{S}_{\mathrm{long}} \right\rangle + \left\langle \vec{S}_{\mathrm{trans}} \right\rangle, \tag{33}$$

where

$$\begin{aligned}\left\langle \vec{S}_{\mathrm{long}} \right\rangle \;=\; & \hat{e}_3\frac{1}{2k^2}\sqrt{\frac{\varepsilon}{\mu}}\,\mathrm{Re}\Big\{\Big(|c_{\mathrm{TE}}|^2+|c_{\mathrm{TM}}|^2\Big)kk_z(\nabla_T\varphi\cdot\nabla_T\varphi^*)\\ & +i\big(c_{\mathrm{TE}}c_{\mathrm{TM}}^*k^2+c_{\mathrm{TE}}^*c_{\mathrm{TM}}k_z^2\big)\Big(\nabla_T^{\perp}\varphi\cdot\nabla_T\varphi^*\Big)\Big\},\end{aligned} \tag{34}$$

and

$$\left\langle \vec{S}_{\mathrm{trans}} \right\rangle = \frac{k_T^2}{2k^2}\sqrt{\frac{\varepsilon}{\mu}}\,\mathrm{Re}\left[-i\left(|c_{\mathrm{TE}}|^2\,\varphi^*\nabla_T\varphi - |c_{\mathrm{TM}}|^2\,\varphi\nabla_T\varphi^*\right)k + c_{\mathrm{TE}}^*c_{\mathrm{TM}}k_z\nabla_T^{\perp}\left(\varphi\varphi^*\right)\right]. \tag{35}$$

As we mention above, a diffraction free beam is such that the divergence of $\langle\vec{S}_{\mathrm{trans}}\rangle$ is zero [30]. If we take the divergence of expression (35), we will get the terms $\nabla\cdot(\varphi^*\nabla_T\varphi)$ and $\nabla\cdot(\varphi\nabla_T\varphi^*)$ which are equal, and as one is the complex conjugate of the other, they must be real, so $\mathrm{Re}[-i(|c_{\mathrm{TE}}|^2\varphi^*\nabla_T\varphi - |c_{\mathrm{TM}}|^2\varphi\nabla_T\varphi^*)] = 0$. Also $\nabla\cdot\nabla_T^{\perp}(\varphi\varphi^*)$ is shown to be equal to zero, as ∇ and $\nabla_T^{\perp}$ are orthogonal. In summary, $\nabla\cdot\langle\vec{S}_{\mathrm{trans}}\rangle = 0$, so, following [30], these beams are diffraction free; physically this means that the time averaged energy flux in the transverse direction is null. Of course, it is possible to calculate explicitly the transversal part of the Poynting vector in each of the four coordinate systems where we have separability into transversal and longitudinal parts (Cartesian, cylindrical, parabolic cylindrical and elliptic cylindrical) and take the divergence; that work had been done explicitly in the four cases, and zero has been obtained.

4.1. Poynting Vector for Bessel Beams

We illustrate the previous results calculating the Poynting vector for Bessel beams of order ν, and we get

$$\left\langle \vec{S}_r \right\rangle = \sqrt{\frac{\varepsilon}{\mu}}\frac{k_T^2}{2kr}\mathrm{Re}\Big\{i\left(|c_{\mathrm{TE}}|^2 - |c_{\mathrm{TM}}|^2\right)J_\nu\left(rk_T\right)\left[\nu J_\nu\left(rk_T\right) - rk_TJ_{\nu-1}\left(rk_T\right)\right]\Big\} = 0, \tag{36a}$$

$$\begin{aligned}\left\langle \vec{S}_\theta \right\rangle = & \sqrt{\frac{\varepsilon}{\mu}}\frac{k_T^2}{2k^2r}\mathrm{Re}\left(\left\{\left(|c_{\mathrm{TE}}|^2 + |c_{\mathrm{TM}}|^2\right)k\nu J_\nu^2\left(rk_T\right) + 2c_{\mathrm{TE}}^*\,c_{\mathrm{TM}}k_zJ_\nu\left(rk_T\right)\right.\right.\\ & \left.\left.\left[rk_TJ_{\nu-1}\left(rk_T\right) - \nu J_\nu\left(rk_T\right)\right]\right\}\right),\end{aligned} \tag{36b}$$

$$\begin{aligned}\left\langle \vec{S}_z \right\rangle = & \sqrt{\frac{\varepsilon}{\mu}}\frac{1}{2k^2r^2}\mathrm{Re}\Big(\Big\{\Big(\big(|c_{\mathrm{TE}}|^2+|c_{\mathrm{TM}}|^2\big)kk_z\left[r^2k_T^2J_{\nu-1}^2(rk_T)+2\nu^2J_\nu^2(rk_T)-2\nu rk_TJ_{\nu-1}\left(rk_T\right)J_\nu(rk_T)\right]\\ & +2\left(k^2c_{\mathrm{TE}}\,c_{\mathrm{TM}}^* + k_z^2c_{\mathrm{TE}}^*\,c_{\mathrm{TM}}\right)\nu J_\nu\left(rk_T\right)\left[rk_TJ_{\nu-1}\left(rk_T\right) - \nu J_\nu\left(rk_T\right)\right]\Big\}\Big).\end{aligned} \tag{36c}$$

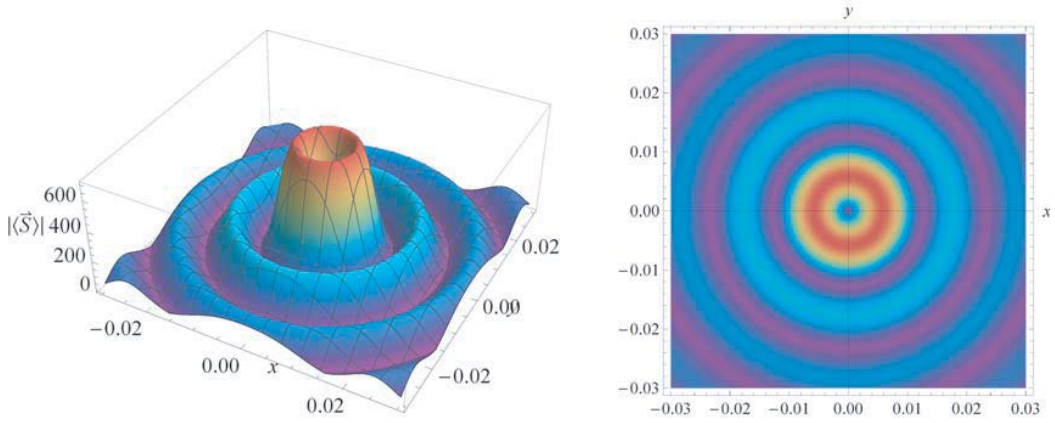

Figure 3. The magnitude of the Poynting vector of a Bessel beam with $\nu = 0$, $k = 630\,\mathrm{m}^{-1}$ and $k_T = 300\,\mathrm{m}^{-1}$. The beam is mixed, it has $c_{\mathrm{TE}} = c_{\mathrm{TM}} = 1$.

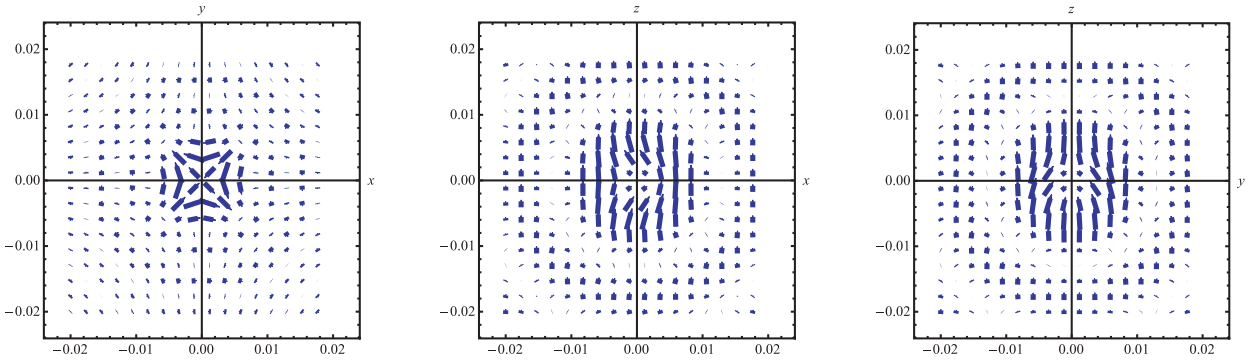

Figure 4. Different projections of the Poynting vector of a Bessel beam of order zero with $k = 630\,\mathrm{m}^{-1}$ and $k_T = 300\,\mathrm{m}^{-1}$. The beam is mixed, it has $c_{\mathrm{TE}} = c_{\mathrm{TM}} = 1$.

The previous equations resemble the component expressions presented for $\vec{S}_\theta$ and $\vec{S}_z$ and the interference part reported in [28]. Note that in this case not only $\nabla \cdot \langle \vec{S}_{\mathrm{trans}} \rangle = 0$, but $\langle \vec{S}_r \rangle = 0$, i.e., we have a zero transversal flux of energy [30].

When $\nu = 0$, we have a zero order Bessel beam, and

$$\left\langle \vec{S}_r \right\rangle = \sqrt{\frac{\varepsilon}{\mu}} \frac{k_T^3}{2k} \mathrm{Re}\left[i J_0\left(k_T r\right) J_1\left(k_T r\right) \left(|c_{\mathrm{TE}}|^2 - |c_{\mathrm{TM}}|^2 \right) \right] = 0, \tag{37a}$$

$$\left\langle \vec{S}_\theta \right\rangle = -\sqrt{\frac{\varepsilon}{\mu}} \frac{k_z k_T^3}{k^2} J_0\left(k_T r\right) J_1\left(k_T r\right) \mathrm{Re}\left(c_{\mathrm{TE}}^* c_{\mathrm{TM}}\right), \tag{37b}$$

$$\left\langle \vec{S}_z \right\rangle = \sqrt{\frac{\varepsilon}{\mu}} \frac{k_z k_T^2}{2k} J_1^2\left(k_T r\right) \left(|c_{\mathrm{TE}}|^2 + |c_{\mathrm{TM}}|^2 \right). \tag{37c}$$

In Figures 3 and 4, we show the Poynting vector of a Bessel beam of zero order with $c_{\mathrm{TE}} = c_{\mathrm{TM}} = 1$. Note that the Poynting vector transversal components circulate the beam center, as reported theoretically [31] and experimentally [32].

5. MAXWELL STRESS TENSOR

Recently, the Maxwell stress tensor has been used to calculate many optical properties of beams, such as angular momentum [33], density flux [34, 35] and counter-propagation vortexes [36]. Some force and torque problems have also been approached using it [37]. Also the scattering of invariants beams for

arbitrary homogeneous dielectric particles (Bessel [38, 39], Weber [40], Mathieu [41]) can be benefited from the employment of this tensor [42]. However, a general formulation in terms of scalar fields has not been presented. Such a presentation can provide new physical insight, apart from simplifying the theoretical treatment by choosing only certain modes for a particular problem and also including "interference between modes".

The Maxwell tensor is a symmetric rank-two tensor, and it is useful to calculate the force interactions when using the Lorentz force is not a suitable alternative. It can be compared to the pressure tensor, where each T_{ij} element can be interpreted as the force per unit of area parallel to the i-th axis suffered by a surface normal to the j-th axis. The diagonal components represent the pressure while the off-diagonal terms can be interpreted as shear stress elements [17]. The time average stress tensor is given by [15–17]

$$\overleftrightarrow{T} = \mathrm{Re}\left[\frac{1}{2}\varepsilon\vec{E}\otimes\vec{E}^{*} + \frac{1}{2}\mu\vec{H}\otimes\vec{H}^{*} - \frac{\vec{E}\cdot\vec{E}^{*}+\vec{H}\cdot\vec{H}^{*}}{4}(\hat{e}_1\otimes\hat{e}_1+\hat{e}_2\otimes\hat{e}_2+\hat{e}_3\otimes\hat{e}_3)\right], \tag{38}$$

where $\otimes$ means the usual outer product, and $\hat{e}_i$, $i = 1, 2, 3$ are the basis orthonormal vectors. After a lengthy calculation, we obtain a general expression for the Maxwell stress tensor,

$$\overleftrightarrow{T} = |c_{\mathrm{TE}}|^2\overleftrightarrow{T}_{\mathrm{TE}} + |c_{\mathrm{TM}}|^2\overleftrightarrow{T}_{\mathrm{TM}} + \overleftrightarrow{T}_{\mathrm{int}}, \tag{39}$$

where

$$\begin{aligned}\overleftrightarrow{T}_{\mathrm{TE}} = \mathrm{Re}\Bigg\{&\frac{\varepsilon}{2k^2}\Big[k_{\mathrm{T}}^4\varphi\varphi^{*}\hat{e}_3\otimes\hat{e}_3 + k^2\nabla_{\mathrm{T}}^{\perp}\varphi\otimes\nabla_{\mathrm{T}}^{\perp}\varphi^{*} + k_z^2\nabla_{\mathrm{T}}\varphi\otimes\nabla_{\mathrm{T}}\varphi^{*} + ik_z{k_{\mathrm{T}}}^2(\varphi^{*}\,\nabla_{\mathrm{T}}\varphi\otimes\hat{e}_3 - \varphi\,\hat{e}_3\otimes\nabla_{\mathrm{T}}\varphi^{*})\Big]\\ &-\frac{1}{4}\left[\frac{\varepsilon}{\mu}\frac{1}{k^2}\left(k_{\mathrm{T}}^4\varphi\varphi^{*} + k_z^2\nabla_{\mathrm{T}}\varphi\cdot\nabla_{\mathrm{T}}\varphi^{*}\right) + \nabla_{\mathrm{T}}^{\perp}\varphi\cdot\nabla_{\mathrm{T}}^{\perp}\varphi^{*}\right]\overleftrightarrow{I}\Bigg\}\end{aligned} \tag{40}$$

is the transversal electric stress tensor,

$$\begin{aligned}\overleftrightarrow{T}_{\mathrm{TM}} = \mathrm{Re}\Bigg\{&\frac{\varepsilon}{2k^2}\Big[k_{\mathrm{T}}^4\varphi\varphi^{*}\hat{e}_3\otimes\hat{e}_3 + k^2\nabla_{\mathrm{T}}^{\perp}\varphi\otimes\nabla_{\mathrm{T}}^{\perp}\varphi^{*} + k_z^2\nabla_{\mathrm{T}}\varphi\otimes\nabla_{\mathrm{T}}\varphi^{*} + ik_z{k_{\mathrm{T}}}^2(\varphi^{*}\,\nabla_{\mathrm{T}}\varphi\otimes\hat{e}_3 - \varphi\,\hat{e}_3\otimes\nabla_{\mathrm{T}}\varphi^{*})\Big]\\ &-\frac{1}{4}\left[\frac{1}{k^2}\left(k_{\mathrm{T}}^4\varphi\varphi^{*} + k_z^2\nabla_{\mathrm{T}}\varphi\cdot\nabla_{\mathrm{T}}\varphi^{*}\right) + \frac{\varepsilon}{\mu}\nabla_{\mathrm{T}}^{\perp}\varphi\cdot\nabla_{\mathrm{T}}^{\perp}\varphi^{*}\right]\overleftrightarrow{I}\Bigg\}\end{aligned} \tag{41}$$

is the transversal magnetic stress tensor, and

$$\begin{aligned}\overleftrightarrow{T}_{\mathrm{int}} = \mathrm{Re}\Bigg\{&\left(c_{\mathrm{TE}}c_{\mathrm{TM}}^{*} + c_{\mathrm{TE}}^{*}c_{\mathrm{TM}}\right)\frac{\varepsilon}{2k}\Big[-k_{\mathrm{T}}^2\left(\varphi\,\hat{e}_3\otimes\nabla_{\mathrm{T}}^{\perp}\varphi^{*} + \varphi^{*}\nabla_{\mathrm{T}}^{\perp}\varphi\otimes\hat{e}_3\right) + ik_z\left(\nabla_{\mathrm{T}}^{\perp}\varphi\otimes\nabla_{\mathrm{T}}\varphi^{*} - \nabla_{\mathrm{T}}\varphi\otimes\nabla_{\mathrm{T}}^{\perp}\varphi^{*}\right)\Big]\\ &-\frac{k_z}{4k}\left[i\left(c_{\mathrm{TE}}c_{\mathrm{TM}}^{*} + \frac{\varepsilon}{\mu}c_{\mathrm{TE}}^{*}c_{\mathrm{TM}}\right)\nabla_{\mathrm{T}}^{\perp}\varphi\cdot\nabla_{\mathrm{T}}\varphi^{*} - i\left(\frac{\varepsilon}{\mu}c_{\mathrm{TE}}c_{\mathrm{TM}}^{*} + c_{\mathrm{TE}}^{*}c_{\mathrm{TM}}\right)\nabla_{\mathrm{T}}\varphi\cdot\nabla_{\mathrm{T}}^{\perp}\varphi^{*}\right]\overleftrightarrow{I}\Bigg\}\end{aligned} \tag{42}$$

is the "interference" stress tensor.

5.1. Maxwell Stress Tensor in Cylindrical Coordinates

Using (15) in the expression that we have obtained for the Maxwell stress tensor, we find the following components

$$\begin{aligned}T_{1,1} \;=\; &\frac{|c_{\mathrm{TE}}|^2}{4k^2\mu r^2}\Big\{2\nu^2J_\nu^2\left(rk_T\right)\left[(\varepsilon-1)k^2\mu + \varepsilon(\mu-1)k_z^2\right] - \varepsilon r^2k_T^4J_\nu^2\left(rk_T\right)\\ &+2\nu rk_TJ_{\nu-1}\left(rk_T\right)J_\nu\left(rk_T\right)\left[k^2\mu + (\varepsilon-2\varepsilon\mu)k_z^2\right] - r^2k_T^2J_{\nu-1}^2\left(rk_T\right)\left[k^2\mu + (\varepsilon-2\varepsilon\mu)k_z^2\right]\Big\}\\ &+\frac{|c_{\mathrm{TM}}|^2}{4k^2\mu r^2}\Big\{2\nu^2J_\nu^2\left(rk_T\right)\left[\varepsilon k^2(\mu-1) + (\varepsilon-1)\mu k_z^2\right] - \mu r^2k_T^4J_\nu^2\left(rk_T\right)\\ &+2\nu rk_TJ_{\nu-1}\left(rk_T\right)J_\nu\left(rk_T\right)\left[\varepsilon k^2 + (\mu-2\varepsilon\mu)k_z^2\right] - r^2k_T^2J_{\nu-1}^2\left(rk_T\right)\left[\varepsilon k^2 + (\mu-2\varepsilon\mu)k_z^2\right]\Big\}\\ &+\left(c_{\mathrm{TE}}\,c_{\mathrm{TM}}^{*} + c_{\mathrm{TE}}^{*}\,c_{\mathrm{TM}}\right)\frac{k_z}{2k\mu r^2}\Big\{\big[\varepsilon(2\mu-1)-\mu\big]\nu J_\nu\left(rk_T\right)\big[rk_TJ_{\nu-1}\left(rk_T\right) - \nu J_\nu\left(rk_T\right)\big]\Big\},\end{aligned} \tag{43}$$

$$
\begin{aligned}
T_{2,2} \;=\; & \frac{|c_{\mathrm{TE}}|^2}{4k^2\mu r^2}\Big\{2\nu^2 J_\nu^2\left(rk_T\right)\left[(\varepsilon-1)k^2\mu+\varepsilon(\mu-1)k_z^2\right]-\varepsilon r^2k_T^4J_\nu^2\left(rk_T\right)\\
& +2\nu rk_TJ_{\nu-1}\left(rk_T\right)J_\nu\left(rk_T\right)\left[(1-2\varepsilon)k^2\mu+\varepsilon k_z^2\right]+r^2k_T^2J_{\nu-1}^2\left(rk_T\right)\left[(2\varepsilon-1)k^2\mu-\varepsilon k_z^2\right]\Big\}\\
& +\frac{|c_{\mathrm{TM}}|^2}{4k^2\mu r^2}\Big\{2\nu^2 J_\nu^2\left(rk_T\right)\left[\varepsilon k^2(\mu-1)+(\varepsilon-1)\mu k_z^2\right]-\mu r^2k_T^4J_\nu^2\left(rk_T\right)\\
& +2\nu rk_TJ_{\nu-1}\left(rk_T\right)J_\nu\left(rk_T\right)\left[\varepsilon k^2(1-2\mu)+\mu k_z^2\right]+r^2k_T^2J_{\nu-1}^2\left(rk_T\right)\left[\varepsilon k^2(2\mu-1)-\mu k_z^2\right]\Big\}\\
& +\left(c_{\mathrm{TE}}\,c_{\mathrm{TM}}^*+c_{\mathrm{TE}}^*\,c_{\mathrm{TM}}\right)\frac{k_z}{2k\mu r^2}\Big\{\left[\varepsilon(2\mu-1)-\mu\right]\nu J_\nu(rk_T)\left[rk_TJ_{\nu-1}(rk_T)-\nu J_\nu\left(rk_T\right)\right]\Big\}, \qquad (44)
\end{aligned}
$$

$$
\begin{aligned}
T_{3,3} \;=\; & \frac{|c_{\mathrm{TE}}|^2}{4k^2\mu r^2}\Big\{J_\nu^2\left(rk_T\right)\left[\varepsilon(2\mu-1)r^2k_T^4-2\nu^2\left(k^2\mu+\varepsilon k_z^2\right)\right]-r^2k_T^2\left(k^2\mu+\varepsilon k_z^2\right)J_{\nu-1}^2\left(rk_T\right)\\
& +2\nu rk_T\left(k^2\mu+\varepsilon k_z^2\right)J_{\nu-1}\left(rk_T\right)J_\nu\left(rk_T\right)\Big\}\\
& +\frac{|c_{\mathrm{TM}}|^2}{4k^2\mu r^2}\Big\{J_\nu^2\left(rk_T\right)\left[(2\varepsilon-1)\mu r^2k_T^4-2\nu^2\left(\varepsilon k^2+\mu k_z^2\right)\right]-r^2k_T^2\left(\varepsilon k^2+\mu k_z^2\right)J_{\nu-1}^2\left(rk_T\right)\\
& +2\nu rk_T\left(\varepsilon k^2+\mu k_z^2\right)J_{\nu-1}\left(rk_T\right)J_\nu\left(rk_T\right)\Big\}\\
& +\left(c_{\mathrm{TE}}\,c_{\mathrm{TM}}^*+c_{\mathrm{TE}}^*\,c_{\mathrm{TM}}\right)\frac{k_z}{2k\mu r^2}\Big\{\nu(\varepsilon+\mu)k_zJ_\nu\left(rk_T\right)\left[\nu J_\nu\left(rk_T\right)-rk_TJ_{\nu-1}\left(rk_T\right)\right]\Big\}, \qquad (45)
\end{aligned}
$$

$$
T_{1,2} \;=\; T_{2,1}=0, \qquad (46)
$$

$$
T_{1,3} \;=\; T_{3,1}=0, \qquad (47)
$$

$$
\begin{aligned}
T_{2,3} \;=\; & T_{3,2}=-\left(|c_{\mathrm{TE}}|^2+|c_{\mathrm{TM}}|^2\right)\frac{k_T^2k_z}{2k^2r}\varepsilon\nu J_\nu^2\left(rk_T\right)\\
& +\left(c_{\mathrm{TE}}\,c_{\mathrm{TM}}^*+c_{\mathrm{TE}}^*\,c_{\mathrm{TM}}\right)\frac{k_T^2}{2kr}\varepsilon J_\nu\left(rk_T\right)\left[\nu J_\nu\left(rk_T\right)-rk_TJ_{\nu-1}\left(rk_T\right)\right]. \qquad (48)
\end{aligned}
$$

In the case of zero-order Bessel beam ($\nu=0$), we get

$$
\begin{aligned}
T_{1,1} \;=\; & |c_{\mathrm{TE}}|^2\frac{k_T^2}{4k^2\mu}\Big\{J_1^2\left(rk_T\right)\left[\varepsilon(2\mu-1)k_z^2-k^2\mu\right]-\varepsilon k_T^2J_0^2\left(rk_T\right)\Big\}\\
& +|c_{\mathrm{TM}}|^2\frac{k_T^2}{4k^2\mu}\Big\{-J_1^2\left(rk_T\right)\left[\varepsilon k^2+(1-2\varepsilon)\mu k_z^2\right]-\mu k_T^2J_0^2\left(rk_T\right)\Big\}, \qquad (49)
\end{aligned}
$$

$$
\begin{aligned}
T_{2,2} \;=\; & |c_{\mathrm{TE}}|^2\frac{k_T^2}{4k^2\mu}\Big\{-J_1^2\left(rk_T\right)\left[(1-2\varepsilon)k^2\mu+\varepsilon k_z^2\right]-\varepsilon k_T^2J_0^2\left(rk_T\right)\Big\}\\
& +|c_{\mathrm{TM}}|^2\frac{k_T^2}{4k^2\mu}\Big\{J_1^2\left(rk_T\right)\left[\varepsilon k^2(2\mu-1)-\mu k_z^2\right]-\mu k_T^2J_0^2\left(rk_T\right)\Big\}, \qquad (50)
\end{aligned}
$$

$$
\begin{aligned}
T_{3,3} \;=\; & |c_{\mathrm{TE}}|^2\frac{k_T^2}{4k^2\mu}\Big\{\varepsilon(2\mu-1)k_T^2J_0^2\left(rk_T\right)-J_1^2\left(rk_T\right)\left(k^2\mu+\varepsilon k_z^2\right)\Big\}\\
& +|c_{\mathrm{TM}}|^2\frac{k_T^2}{4k^2\mu}\Big\{(2\varepsilon-1)\mu k_T^2J_0^2\left(rk_T\right)-J_1^2\left(rk_T\right)\left(\varepsilon k^2+\mu k_z^2\right)\Big\}, \qquad (51)
\end{aligned}
$$

$$
T_{1,2} \;=\; T_{2,1}=0, \qquad (52)
$$

$$
T_{1,3} \;=\; T_{3,1}=0, \qquad (53)
$$

$$
T_{2,3} \;=\; T_{3,2}=\left(c_{\mathrm{TE}}c_{\mathrm{TM}}^*+c_{\mathrm{TE}}^*c_{\mathrm{TM}}\right)\frac{k_T^3}{2k}\varepsilon J_0\left(rk_T\right)J_1\left(rk_T\right). \qquad (54)
$$

6. AN EXAMPLE. THE FORCE OVER A CYLINDER

In order to show and emphasize the utility of the Maxwell stress tensor, let us calculate the electromagnetic force over a small cylinder on which a transversal electric ($c_{\mathrm{TM}} = 0$) impinges a zero-order Bessel field. The electromagnetic force is given in this case by [15–17]

$$F = \oint_S \overleftrightarrow{T} \cdot \vec{da}. \tag{55}$$

The Maxwell stress tensor reduces to ($c_{\mathrm{TE}} = 1$ and $c_{\mathrm{TM}} = 0$)

$$T_{1,1} = \frac{k_T^2}{4k^2\mu}\Big\{ J_1^2\left(rk_T\right)\left[\varepsilon(2\mu-1)k_z^2 - k^2\mu\right] - \varepsilon k_T^2 J_0^2\left(rk_T\right)\Big\}, \tag{56}$$

$$T_{2,2} = \frac{k_T^2}{4k^2\mu}\Big\{ - J_1^2\left(rk_T\right)\left[(1-2\varepsilon)k^2\mu + \varepsilon k_z^2\right] - \varepsilon k_T^2 J_0^2\left(rk_T\right)\Big\}, \tag{57}$$

$$T_{3,3} = \frac{k_T^2}{4k^2\mu}\Big\{\varepsilon(2\mu-1)k_T^2 J_0^2\left(rk_T\right) - J_1^2\left(rk_T\right)\left(k^2\mu + \varepsilon k_z^2\right)\Big\}, \tag{58}$$

$$T_{1,2} = T_{2,1} = T_{1,3} = T_{3,1} = T_{2,3} = T_{3,2} = 0. \tag{59}$$

We consider that the axis of the cylinder coincides with the Z axis has a longitude $2L$ and radius R. The integrals over the two plane circular surfaces cancel each other and the integral over the curved side gives the following pressure in the radial direction

$$\mathcal{P} = \frac{k_T^2}{4k^2\mu}\left\{\left[\varepsilon\left(2\mu-1\right)k_z^2 - \mu k^2\right] J_1^2\left(k_T R\right) - \varepsilon k_T^2 J_0^2\left(k_T R\right)\right\}. \tag{60}$$

This pressure can be positive (directed outside) or negative (directed inside) depending on the parameters.

7. CONCLUSIONS

We have shown how to obtain the principal properties for invariant propagation beams such as plane wave, Bessel, Mathieu and Weber. Based on the scalar approach, we provide general expressions for energy density, Poynting vector and Maxwell stress tensor. In fact, these results can be used to study the orbital angular momentum of nonparaxial beams [43] and new optical phenomena, where these fields are present. Additionally, there are analytical expressions to study the interaction between modes, as in [28]. Furthermore, the scalar formalism can invite researchers to calculate electromagnetic properties for any new optical field not discovered yet but written in a scalar form [18]. The present results should be of interest to a wide audience due to its fundamental character.

ACKNOWLEDGMENT

We acknowledge the ideas and supervision of B. M. Rodríguez-Lara during the first stage of research and are grateful for his continuous support and enlightening discussion. IRO acknowledges financial support from CONACYT graduate studies grant 423320.

REFERENCES

1. Durnin, J., "Exact solutions for nondiffracting beams. I. The scalar theory," *J. Opt. Soc. Am. A*, Vol. 4, No. 4, 651–654, 1987.
2. Gutiérrez-Vega, J. C., M. D. Iturbe-Castillo, and S. Chávez-Cerda, "Alternative formulation for invariant optical fields: Mathieu beams," *Opt. Letters*, Vol. 25, No. 20, 1493–1495, 2000.
3. Bandres, M. A., J. C. Gutiérrez-Vega, and S. Chávez-Cerda, "Parabolic nondiffracting optical wave fields," *Opt. Letters*, Vol. 29, No. 1, 44–46, 2004.

4. Jáuregui, R. and S. Hacyan, "Quantum-mechanical properties of Bessel beams," *Phys. Rev. A*, Vol. 71, No. 033411, 2005.
5. Rodríguez-Lara, B. M. and R. Jáuregui, "Dynamical constants for electromagnetic fields with elliptic-cylindrical symmetry," *Phys. Rev. A*, Vol. 78, No. 033813, 2008.
6. Rodríguez-Lara, B. M. and R. Jáuregui, "Dynamical constants of structured photons with parabolic-cylindrical symmetry," *Phys. Rev. A*, Vol. 79, No. 055806, 2009.
7. Rodríguez-Lara, B. M. and R. Jáuregui, "Single structured light beam as an atomic cloud splitter," *Phys. Rev. A*, Vol. 80, No. 011813R, 2009.
8. Zhang, L. and P. L. Marston, "Optical theorem for acoustic non-diffracting beams and application to radiation force and torque," *Biomed. Opt. Express*, Vol. 4, No. 9, 1610–1617, 2013.
9. Wulle, T. and S. Herminghaus, "Nonlinear optics of Bessel beams," *Phys. Rev. Lett.*, Vol. 71, No. 209, 1401–1404, 1993.
10. Ambrosio, L. A. and H. E. Hernández-Figueroa, "Integral localized approximation description of ordinary Bessel beams and application to optical trapping forces," *Biomed. Opt. Express*, Vol. 2, No. 7, 1893–1906, 2011.
11. Blonskyi, I., V. Kadan, I. Dmitruk, and P. Korenyuk, "Cherenkov phase-matching in Raman-seeded four-wave mixing by a femtosecond Bessel beam," *Appl. Phys. B*, Vol. 107, 649–652, 2012.
12. Willner, A. E., et al., "Optical communications using orbital angular momentum beams," *Adv. Opt. Photon.*, Vol. 7, No. 1, 66–106, 2015.
13. Volke-Sepulveda, K., S. Garces-Chavez, S. Chávez-Cerda, J. Arlt, and K. Dholakia, "Orbital angular momentum of a high-order Bessel light beam," *J. Opt. B: Quantum Semiclass. Opt.*, Vol. 4, S82–S89, 2002.
14. Volke-Sepulveda, K. and E. Ley-Koo, "General construction and connections of vector propagation invariant optical fields: TE and TM modes and polarization states," *J. Opt. A: Pure Appl. Opt.*, Vol. 8, No. 10, 867–877, 2006.
15. Stratton, J. A., *Electromagnetic Theory*, McGraw-Hill, 1941.
16. Jackson, J. D., *Classic Electrodynamics*, 3rd Edition, Wiley, 1999.
17. Griffiths, D. J., *Introduction to Electrodynamics*, 3rd Edition, Prentice Hall, 1999.
18. Boyer, C. P., E. G. Kalnins, and W. Miller, Jr., "Symmetry and separation of variables for the Helmholtz and Laplace equations," *Nagoya Math. J.*, Vol. 60, 35–80, 1976.
19. Bouchal, Z., "Nondiffracting optical beams: Physical properties, experiments, and applications," *Czechoslovak Journal of Physics*, Vol. 53, 537–578, 2003.
20. Gutiérrez-Vega, J. C., R. Rodriguez-Dagnino, M. Meneses-Nava, and S. Chávez-Cerda, "Mathieu functions, a visual approach," *Am. J. Phys.*, Vol. 71, No, 3, 233–242, 2003.
21. López-Mariscal, C., M. A. Bandres, J. C. Gutirrez-Vega, and S. Chávez-Cerda, "Observation of parabolic nondiffracting optical fields," *J. Opt. Soc. Am.*, Vol. 13, No. 7, 2364–2369, 2005.
22. Hernández-Figueroa, H. E., M. Zamboni-Rached, and E. Recami, *Non-diffracting Waves*, John Wiley & Sons, 2013.
23. McGloin, D. and D. K. Dholakia, "Bessel beams: Diffraction in a new light," *Contemporary Physics*, Vol. 46, No. 1, 15–28, 2005.
24. Flores-Pérez, A., J. Hernández, R. Jáuregui, and K. Volke-Sepúlveda, "Experimental generation and analysis of first-order TE and TM Bessel modes in free space," *Opt. Letters*, Vol. 31, No. 11, 1732–1734, 2006.
25. Mishra, S., "A vector wave analysis of a Bessel beam," *Opt. Comm.*, Vol. 85, 159–161, 1991.
26. Bouchal, Z. and Z. M. Olivik, "Non-diffractive vector Bessel beams," *J. Modern Opt.*, Vol. 42, 1555–1566, 1995.
27. Yu, Y.-Z. and W.-B. Dou, "Vector analyses of nondifracting beams," *Progress In Electromagnetics Research Letters*, Vol. 5, 57–71, 2008.
28. Novitsky, A. V. and D. V. Novitsky, "Negative propagation of vector Bessel beams," *Opt. Soc. Am. A*, Vol. No. 24, 2844–2849, 2007.

29. Lin, Y., W. Seka, J. Eberly, H. Huang, and D. Brown, "Experimental investigation of Bessel beam characteristics," *Applied Opt.*, Vol. 11, No. 15, 2708–2713, 1992.
30. Bajer, J. and R. Horak, "Nondiffractive fields," *Phys. Rev. E*, Vol. 54, No. 3, 3052–3054, 1996.
31. Litvin, I. A., "The behavior of the instantaneous Poynting vector of symmetrical laser beams," *J. Opt. Soc. Am.*, Vol. 29, No. 6, 901–907, 2012.
32. Mokhun, I., A. Arkhelyuk, Y. Galushko, Y. Kharitonovtta, and J. Viktorovskaya, "Experimental analysis of the Poyting vector characteristics," *Applied Opt.*, Vol. 51, No. 10, C158–C162, 2012.
33. Allen, L., M. W. Beijersbergen, R. J. C. Spreeuw, and J. Woerdman, "Orbital angular momentum of light and the transformation of Laguerre-Gaussian lases modes," *Phys. Rev. A*, Vol. 45, No. 11, 8185–8189, 1992.
34. Barnett, S. M. and L. Allen, "Orbital angular momentum and nonparaxial light beams," *Opt. Comm.*, Vol. 110, 670–678, 1994.
35. Barnett, S. M., "Optical angular momentum flux," *J. Opt. B: Quantum and Semiclass. Optics*, Vol. 4, S7–S16, 2002.
36. Mitri, F. G., "Counterpropagating nondifracting vortex beams with linear and angular momenta," *Phys. Rev. A*, Vol. 88, 035804, 2013.
37. Barton, J. P., D. R. Alexander, and S. A. Schaub, "Theoretical determination of net radiation force and torque for a spherical particle illuminated by a focused laser beam," *J. Appl. Phys.*, Vol. 66, 4594–4602, 1989.
38. Marston, P. L., "Scattering of a Bessel beam by sphere," *J. Acoust. Soc. Am.*, Vol. 121, No. 2, 753–758, 2007.
39. Marston, P. L., "Scattering of a Bessel beam by sphere II: Helicoidal case shell example," *J. Acoust. Soc. Am.*, Vol. 124, No. 5, 2905–2910, 2008.
40. Belafhal, A., A. Chafiq, and Z. Hricha, "Scattering of Mathieu beams by a rigid sphere," *Opt. Comm.*, Vol. 284, 3030–3035, 2011.
41. Belafhal, A., L. Ez-Zariy, A. Chafiq, and Z. Hricha, "Analysis of the scattering far field of a nondiffracting parabolic beam by a rigid sphere," *Phys. and Chem. News*, Vol. 60, 15–21, 2011.
42. Cui, Z., Y. Han, and L. Han, "Scattering of a zero-order Bessel beam by shaped homogeneous dielectric particles," *J. Opt. Soc. Am. A*, Vol. 30, No. 10, 1913–1920, 2013.
43. Brandao, P., "Nonparaxial TE and TM vector beams with well-defined orbital angular momentum," *Opt. Letters*, Vol. 37, No. 5, 909–911, 2012.